

Diffusion Layer Growth and Compound Formation Sequence of Titanium-Carbon Steel Tri-metal Composite (Ti-Ni-steel) Sheets Fabricated by Hot-roll Diffusion Bonding

Chun-Ming Lin*

Keywords : Diffusion layer growth, Compound formation, Tri-metal composite sheets, Hot-rolling, Diffusion bonding.

ABSTRACT

The primary objective in this work was to investigate the diffusion layer growth and compound formation sequence of titanium-carbon steel tri-metal composite sheets fabricated. Those results give a useful insight into the effects of different processing temperatures on the interface evolution at the Ti/Ni interface in hot-roll diffusion-bonded Ti/Ni/ steel joints, and observations of microstructure and thermodynamic calculations revealed some interesting results. During the diffusion process, Ni_3Ti and NiTi_2 begin nucleation at nearly the same time; therefore, the thickness of the two layers was very similar. Finally, Ti and Ni diffuse to the interface between the NiTi_2 and Ni_3Ti compound layers to form NiTi. As the thickness of the NiTi layer increases, part of Ni_3Ti is consumed; leading to a reduction in its thickness, it can be attributed to the lower reaction Gibbs free energies and surface energy increments of Ni_3Ti and NiTi_2 . The $\alpha + \beta$ Ti phases additionally exist as discrete needle-shaped particles in the matrix of Ni_3Ti phase, while β -Ti phases exist as discrete islands in the matrix of NiTi_2 phase. The presence of Ni in the interfacial zone adjacent to the Ti substrate stabilizes β -Ti phase, leads to the formation of needle-shaped $\alpha + \beta$ -Ti phase.

INTRODUCTION

The light weight, high strength-to-weight ratio, high toughness, high creep resistance and excellent corrosion resistance of titanium (Ti) alloys have led to their extensive use in the aerospace,

Paper Received June, 2019. Revised September, 2019. Accepted October, 2019. Author for Correspondence: Chun-Ming Lin.

* Assistant Professor, Department of Mechanical Engineering, Minghsin University of Science and Technology, Hsinchu, 30401, Taiwan.

In many applications, it is necessary to bond the Ti with some other metal or alloy in order to achieve the desired functional performance [3] and the potential they provide. However, Ti is extremely reactive at high temperatures, and hence the bonding process represents a significant challenge since the Ti readily reacts with oxygen and / or nitrogen in the atmosphere [4,5]. To improve the practical applicability of Ti-steel sheet (SS) bonded joints, it is necessary to increase their plasticity by reducing the volume fraction of intermetallic compounds (IMCs) using some form of solid-state connection method or selecting a suitable interlayer material. The use of hot-roll diffusion bonding to form dissimilar joints has attracted significant attention in the recent literature [6-10]. The hot rolling process provides an effective means of joining similar or dissimilar materials without gross microscopic distortion [11,12]. However, the interfacial strength of such diffusion bonding specimen is heavily dependent on their microstructural evolution during the bonding process. The evolution process is dependent in turn on the temperature at which rolling is performed. Therefore, it is essential to confirm the quantitative relationships among the diffusion-controlled reaction properties, rolling temperature, and hot deformation behavior of the constituent materials in the hot-rolling process. However, the literature contains relatively little information on the effects of the processing temperature on the interfacial microstructural evolution (i.e., diffusion layer growth and compound formation sequence) of hot-roll diffusion bonded joints with interlayer. Accordingly, the present study sets out to investigate the effects of the diffusion temperature on the interfacial microstructural evolution of Ti-SS composite sheets containing a nickel interlayer fabricated by the hot-roll diffusion bonding process at temperatures of 800, 850 and 900°C, respectively. The joints produced under the different bonding temperatures are characterized both experimentally and through thermodynamic analyses based on the Gibbs free energy of reaction and interface energy theory. The results give a useful

theoretical insight into the effects of the processing temperature on the interface evolution at the Ti/Ni interface in hot-roll diffusion-bonded Ti/Ni/SS joints and are thus expected to provide a valuable source of reference for the fabrication of such joints in engineering and other fields.

EXPERIMENTAL PROCEDURE

The hot-roll diffusion bonding trials were performed using pure Ti and carbon steel plates with dimensions of 150 mm × 100 mm × 16.2 mm, in fabricating the joints for the two plates were separated by a pure Ni (99.95%) interlayer (note that prior to the bonding process, the Ti and carbon steel plates were cleaned with emery paper and then scratch brushed with pure Ti and carbon steel circumferential brushes, respectively, in order to remove the oxidization layers. The edges of the two plates were then mechanically cleaned with abrasive paper. Finally, the plates were placed in an acetone-containing vessel and degreased ultrasonically for 20 minutes. Test specimens were assembled by inserting the Ni foil between the two plate). The specimens were placed in a furnace for 600 s (i.e., pre-heated) at 450°C, and then multi pass continuous hot rolling process was applied using a rolling mill and then roll-bonded to achieve a final thickness reduction of approximately 45% (i.e., tri-metal composite (Ti-Ni-steel) sheets from an initial thickness of 16.2 mm to a final thickness of approximately 11.34 mm) at 800°C, 850°C or 950°C in 5 passes, that the rolling reductions of approximately 5%, 15%, 25%, 35% and 45% were obtained with the rolling speed of 0.2 m/s. The roll bonding was performed on a laboratory rolling mill with rolls of 170 mm in diameter and 300 mm in width without lubrication at a rolling speed of 0.2 m/s. The rolling process was conducted in an inert atmosphere (high purity argon gas (99.99%)) to inhibit oxidation of the rolled interface (see Fig. 1).

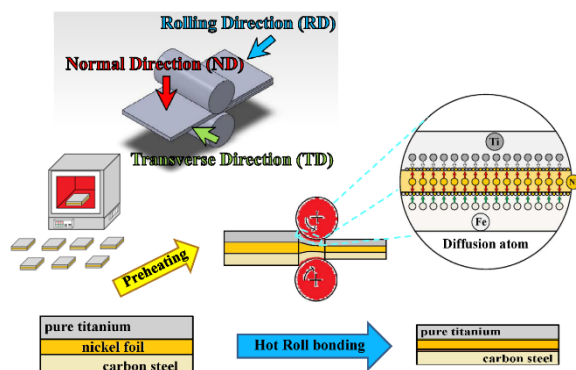


Fig. 1. Schematic illustration showing structure of hot-roll diffusion bonded joints.

Following the rolling process, the specimens were allowed to cool naturally to room temperature in the furnace and were then annealed at 550°C in a muffle furnace for 3 hr (i.e., in an inert atmosphere (high purity nitrogen gas (99.999%))) to reduce the stress concentration. The specimens were etched in 3% Nital solution and Kroll's solution for 45 s to reveal the cross-sectional microstructure. The interfacial regions of the joints were analyzed using a scanning electron microscope (SEM, JEOL JSM-5410). In addition, the chemical compositions and element distributions were examined using energy dispersive X-ray spectrometry (EDS).

RESULTS AND DISCUSSION

Fig. 2(a) to (c) present SEM cross-sectional images of the tri-metal composite (Ti-Ni-steel) samples diffusion bonded at temperatures of 800, 850 and 900°C, respectively. For all three samples, the diffusion interface between the carbon steel plate and the Ni interlayer shows some defects, discontinuities, and voids. In the sample diffusion bonded at 800°C, the interfacial region between the Ti plate and the Ni interlayer also shows obvious defects (i.e., discontinuities and voids). However, these defects are less evident in the samples processed at higher temperatures of 850 and 900°C, respectively. The SEM images in Fig. 2 confirm that a higher bonding diffusion temperature results in a greater diffusion layer thickness. At a lower bonding temperature (800°C, Fig. 2(a)), the compound layers have the form of isolated phases and are present in only relatively small amounts. However, as the bonding temperature increases, the number of compound layers increases and discrete reaction layers are formed (see Figs. 2(b) and 2(c)). In particular, the pure Ti-Ni interlayer interface region contains a NiTi₂ compound layer (i.e., dark-gray region) adjacent to the Ti plate and a Ni₃Ti compound layer (i.e., gray-white region) adjacent to the Ni interlayer. The two compound layers are separated by a NiTi compound layer (i.e., gray region) (see Fig. 2(c), for example). This finding is reasonable since the use of a Ni interlayer harmonizes the rolling temperature, and consequently increases the strain value of the Ti-Ni diffusion interface. The higher strain value at the Ti-Ni diffusion interface increases the dislocation density and stored energy in the Ni interlayer [13] and therefore increases the diffusion layer thickness width of the Ti-Ni interface. Moreover, according to the dislocation hypothesis [13], dislocations at free surfaces undergoing plastic deformation break the oxide layers and produce stairs at the atomic scale, which increase the involvement of the diffusion bonded joint parts. In addition, the Ni-carbon steel interface is thus free from any reaction products for bonding temperatures of 800~900°C.

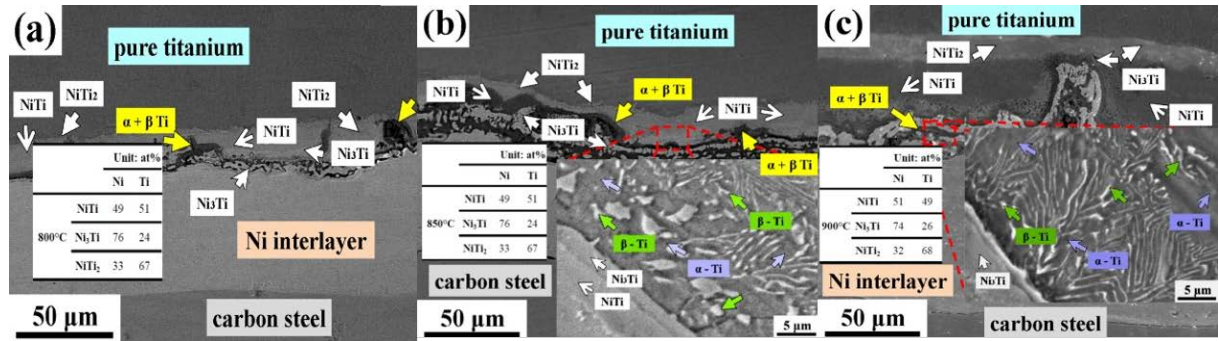


Fig. 2. Backscattered electron (BE) images of cross-sectional regions of pure Ti and carbon steel hot-roll diffusion bonded joints with Ni interlayer processed at temperatures of: (a) 800°C, (b) 850°C and (c) 900°C.

According to [14-16] reports, the formation process for the NiTi_2 and Ni_3Ti phases can be elaborated as follows. Under the effects of the elevated bonding temperature, a NiTi compound layer is rapidly formed during the initial stage of the bonding process due to the relatively low diffusion speeds of Ti and Ni, respectively. However, due to the strong affinity of the Ti-Ni atom pairs (i.e., a relatively high degree of negative mixing enthalpy of the principal elements in the alloy system), the Ni atoms diffuse very quickly toward the Ti layer (i.e., β -Ti) [17]. As the diffusion of Ni atoms proceeds, β -Ti phase begins to form as a result of isothermal transformation, i.e., $\alpha + \beta\text{-Ti} \rightarrow \beta\text{-Ti}$, in accordance with the Ti-Ni binary phase diagram [18]. As the holding time increases, the inward diffusion of Ni atoms also increases. Moreover, the α -Ti phase transforms to NiTi_2 compound through the isothermal reaction $\beta\text{-Ti} \rightarrow \text{NiTi}_2$ owing to the similarity in the crystal structures and compositions of NiTi and NiTi_2 , respectively. The β -Ti phase and disordered α -Ti phase dissolve a greater amount of Ni than the ordered NiTi_2 compound. As a result, excess dissolved Ni is expelled from the NiTi_2 phase. The segregated Ni atoms combine with the Ni atoms diffused from the Ti substrate to form Ni_3Ti compound. Thus, a continuous NiTi_2 compound with almost no Ni is formed adjacent to the TiNi_3 compound. The Ni_3Ti phase has a higher chemical affinity than the NiTi_2 phase, and hence a difference in the chemical potential is produced between them. Consequently, NiTi_2 compound precipitates are formed in the α -Ti matrix in accordance with the eutectoid reaction $\beta\text{-Ti} \rightarrow \alpha\text{-Ti} + \text{NiTi}_2$ during the cooling process [18-20]. A close inspection of Figs. 2(b) and 2(c) reveals the presence of $\alpha + \beta$ -Ti phases in the form of discrete needle-shaped particles in the matrix of the Ni_3Ti compound and β -Ti phases in the form of discrete islands in the matrix of the NiTi_2 phase in the compound reaction layers. This can be attributed to a relatively high degree of negative mixing enthalpy between Ni-Ti, which leads to the formation and subsequent segregation of atom pairs within the matrix.

The images presented in Fig. 2 show that NiTi_2 ,

NiTi and Ni_3Ti compounds are formed in the bonded joints as the result of an inter-diffusion of the Ti and Ni elements during the bonding process. The associated chemical reactions can be formulated as follows:



where s represents the solid state. Based on classical nucleation theory, the nucleation of a new phase involves changes of the Gibbs free energies of reaction (ΔG_f) and interfacial energies (γ), respectively. When the element substances become compound phases as a result of heat treatment, welding, hot-roll bonding, and so on, ΔG_f is always negative. Furthermore, a larger absolute value of ΔG_f infers that the associated reaction more readily occurs.

$$\Delta G_{f,AB}(T) = G_{AB}(T) - \sum |v_{ei}| G_{ei}(T), \quad (4)$$

where v_{ei} is the stoichiometric coefficient. The Gibbs free energies of the generated compounds $G_{AB}(T)$ and reactive elements $G_{ei}(T)$ in Eq. (4) can be calculated as follows [21]:

$$G(T) = H(T) - TS(T), \quad (5)$$

$$H(T) = H(298.15) + \int_{298.15}^{T_1} C_{p1}(T) dT + \quad (6)$$

$$\Delta H_{T_1} + \int_{T_1}^{T_2} C_{p2}(T) dT + \Delta H_{T_2} + \dots,$$

$$S(T) = H(298.15) + \int_{298.15}^{T_1} \frac{C_{p1}(T)}{T} dT + \quad (7)$$

$$\frac{\Delta H_{T_1}}{T} + \int_{T_1}^{T_2} \frac{C_{p2}(T)}{T} dT + \frac{\Delta H_{T_2}}{T} + \dots,$$

where $H(T)$ and $S(T)$ are the enthalpy and entropy of the elements or compounds, respectively; and C_P is the heat capacity. C_P is a function of the temperature and can be described by the following polynomial expression over a relatively wide range of temperatures:

$$C_p = a + b \times 10^{-3}T + c \times 10^5 T^{-2} + d \times 10^{-6} T^2, \quad (8)$$

where a , b , c and d are constants obtained from the thermochemical data of pure substances (II) [21].

The calculated values of ΔG_f obtained from Eqs. (5)~(8) for the present NiTi_2 , NiTi and Ni_3Ti compounds are listed in Table 1. It is clear that the ΔG_f values of the three compounds are very different and the ΔG_f values of Ni_3Ti and NiTi_2 are smaller than that of NiTi . Overall, the results indicate that reactions (1)

and (3) occur more readily than reaction (2). In other words, the formation sequence of the intermediate phases is confirmed to be Ni₃Ti, NiTi₂ and TiNi.

Although ΔG_f allows for the immediate assessment of the stability of a substance, it is insufficient to categorically determine the formation sequence of the compound phases. Therefore, the interfacial energy, which plays a decisive role in the early stage of nucleation is introduced here as an alternative evaluation measure. In particular, a compound phase with a smaller interfacial energy increment is assumed to nucleate more readily. In general, the calculation of the interfacial energy increment involves the surface energies of the new compound phases (γ_{AB}) and initial substances (γ_i , $i = A$ or B), the interfacial energy of the initial A/B interface (γ_{A-B}), and the interfacial energy of the new interface A/AB or B/AB (γ_{A-AB} or γ_{B-AB}). (Note that in the present research, AB may be Ni₃Ti, NiTi₂, or NiTi.). The surface energy of the substances can be given empirically as [22]

$$\gamma_A(T_1) = \frac{(\gamma_A V_A^{\frac{2}{3}})^{T=0} + b_A T_1}{(V_A^{\frac{2}{3}})^{T=T_1}}, \quad (9)$$

where $V_A^{T=0}$ is the surface energy of A at $T = 0$ K, which can be estimated by the enthalpy for evaporation of one mole of atoms divided by the atomic surface of one mole of atoms; b_A is a material constant for Ti or Ni (note that $b_{Ti} = -0.47 \times 10^7$ J/K, $b_{Ni} = -0.73 \times 10^7$ J/K) [23], and V_A is the molar volume of Ti or Ni. Meanwhile, the surface energy of the compounds can be calculated as [23,24]

$$\gamma_{AB} = C_A^S \gamma_A + C_B^S \gamma_B - C_A^S C_B^S \frac{\Delta H_{A \text{ in } B}^{\text{interface}}}{C_0 V_A^{\frac{2}{3}}}, \quad (10)$$

where C_A^S and C_B^S are the volume fractions of A and B, respectively; and $\Delta H_{A \text{ in } B}^{\text{interface}}$ is the enthalpy change upon solution of one mole of A in B, as described earlier in relation to Eqs. (1) and (2). In addition, C_0 is a constant depending on the shape of the Wigner-Seitz cell of the A atoms and can be taken on average as $\approx 4.5 \times 10^8$ [25]. The interfacial energy between a solid phase A and solid phase B (i.e., γ_{A-B}) contains two contributions, namely $\gamma_{A-B}^{\text{mismatch}}$ and $\gamma_{A-B}^{\text{interface}}$ [23,26]. In other words, the energy of the A-B interface is given as

$$\gamma_{A-B} = \gamma_{A-B}^{\text{mismatch}} + \gamma_{A-B}^{\text{interface}} = \frac{1}{3} \left(\frac{\gamma_A + \gamma_B}{2} \right) + \frac{\Delta H_{A \text{ in } B}^{\text{interface}}}{C_0 V_A^{\frac{2}{3}}}, \quad (11)$$

where $\gamma_{A-B}^{\text{mismatch}}$ is related to the strain induced by the lattice mismatch at the interface and $\gamma_{A-B}^{\text{interface}}$ is related to the chemical interaction between A and B. Similarly, γ_{A-AB} and γ_{B-AB} can be defined respectively as

$$\gamma_{A-AB} = \frac{1}{3} \left(\frac{\gamma_A + \gamma_{AB}}{2} \right) + \frac{C_B^S \Delta H_{A \text{ in } B}^{\text{interface}}}{C_0 V_A^{\frac{2}{3}}}, \quad (12)$$

$$\gamma_{B-AB} = \frac{1}{3} \left(\frac{\gamma_B + \gamma_{AB}}{2} \right) + \frac{C_A^S \Delta H_{B \text{ in } A}^{\text{interface}}}{C_0 V_B^{\frac{2}{3}}}, \quad (13)$$

The interfacial energy increment of Ni₃Ti, NiTi₂ and NiTi are listed in Table 1, as computed by Eqs. (2) and (3) and Eqs. (9)~(13). Overall, the results show that the Ni₃Ti phase has the smallest interfacial energy increment of the three compounds. Hence, it is inferred that Ni₃Ti has the highest possibility of nucleating first. However, as reported in [27], the formation sequence of the second compound phase also depends on x^{crit} , where x^{crit} is the critical thickness of the first compound phase in the diffusion system. In the Ti-Ni system, two main possibilities exist for the formation mechanism if the supply of A (Ti or Ni) and B (Ni or Ti) is limited, namely (1) x_f (the thickness of the reaction layers) $< x^{\text{crit}}$ when A or B is consumed: the second compound phase nucleates and grows while the first compound phase shrinks; or (2) $x_f \geq x^{\text{crit}}$ before A or B is consumed: the second compound phase nucleates and grows, and the first compound phase continues to grow as well [27]. The present experimental results for Table 2 shown that the Ni/Ti possible formation sequences of the three compounds, the first possible phase formation sequence is as interfacial film considered in the present study, with a thickness of approximately 50 μm , belongs to the second case. That is, before A or B is consumed, the thickness of the first compound phase x_f is higher than the critical thickness and the second compound phase thus forms as the first compound phase continues to grow. According to the interfacial energy theory results presented above, Ni₃Ti appears first in the diffusion process. In other words, the second compound phase could be either NiTi₂ or NiTi. However, according to x^{crit} theory, the NiTi compound can only be nucleated after Ni₃Ti and NiTi₂ have been formed since its nucleation and growth are both dependent on the prior formation of Ni₃Ti and NiTi₂ layers. In other words, Ni₃Ti and NiTi₂ nucleate first and are then followed by NiTi. Such a result Fig. 3 shows the two alternative possible formation sequences of the three compounds, the first possible phase formation sequence is as follows: Ni₃Ti \rightarrow NiTi₂ \rightarrow NiTi, as the interfacial evolution of I \rightarrow II \rightarrow III \rightarrow V shown Fig. 3(a). (Note that I and II represent the original Ti/Ni interface and the interface with only Ni₃Ti formed, respectively, while III denotes the interface with NiTi₂ formed between Ni₃Ti and Ti, and V denotes the interface with all three compounds). Meanwhile, the second possible formation sequence is: I \rightarrow IV \rightarrow V, in which the IV interface is different from the III interface. In particular, IV shown Fig. 3(b) that the interface with Ni₃Ti and NiTi₂ forms almost simultaneously and is then followed by the formation of NiTi. Based on the above results, we speculate that the order of compound formation at the Ti/Ni interface was as follows: I \rightarrow IV \rightarrow V. Our main reason for this assertion is the fact that the thicknesses of Ni₃Ti and

Table 1 Calculated Gibbs free energies (ΔG_f) and interface energies for NiTi, NiTi₂ and Ni₃Ti compounds in Ti-Ni diffusion interface.

		Unit: KJ/mol		
		NiTi	NiTi ₂	Ni ₃ Ti
ΔG_f	800°C (1073K)	-118.3	-730.0	-616.0
	850°C (1123 K)	-117.2	-724.3	-615.1
	900°C (1173 K)	-116.0	-714.2	-614.1
		Unit: mJ/m ²		
		NiTi	NiTi ₂	Ni ₃ Ti
Surface energy ($\gamma_{(AB)}$)		2219.69	2289.21	2176.32
Interface energy (γ_{Ti-AB})		380.63	489.23	168.54
Interface energy (γ_{Ni-AB})		243.31	122.63	443.18
Increasing interface energy		743.32	728.41	725.21
Remarks		$\gamma_{(Ti-Ni)} = -104.25$	$\gamma_{(Ni)} = 2001.9$	$\gamma_{(Ti)} = 2048.2$

Table 2 Thicknesses of NiTi and remnant NiTi layers in samples processed at temperatures of 800, 850 and 900°C.

		Unit: μm							
		800°C		850°C		900°C			
		NiTi	Total	NiTi	Total	NiTi	Total		
Remnant NiTi layers	NiTi	5.8	14.9	NiTi	12.2	29.1	44.3		
	Ni ₃ Ti	5.6		Ni ₃ Ti	6.3			Ni ₃ Ti	8.4
	NiTi ₂	3.5		NiTi ₂	5.8			NiTi ₂	6.8

NiTi₂ were nearly identical, despite differences in processing conditions (See Table 2)

It appears that Ni₃Ti and NiTi₂ formed at almost the same time, rather than Ni₃Ti forming before NiTi₂. We also observed that $\alpha + \beta$ Ti phases exist as discrete needle-shaped particles in the matrix of the Ni₃Ti, whereas β -Ti phases exist as discrete islands in the matrix of the NiTi₂. Note that these results help to clarify many reports dealing with Ti/Ni interfaces, by settling the debate as to the order in which Ni₃Ti, NiTi₂, and NiTi form. Overall, both sets of results indicate an inter-diffusion of the two elements (Ti and Ni). The gradual increase in the Ti concentration from the Ti side to the Ni side of the Ti-Ni joint provides further evidence of diffusion in the bonding process. According to the elemental concentration profiles (see Fig. 4), this interfacial region of the joint consists

mainly of Ti with a small amount of Ni, due to the gradual increase in the Ti concentration from the Ti side to the Ni side of the Ti-Ni joint provides further evidence of diffusion in the bonding process. According to the elemental concentration profiles, this interfacial region of the joint consists mainly of Ti with a small amount of Ni. The Ti and Ni concentration profiles both exhibit smooth and continuous variations. Therefore, it is inferred that Ti solid solution (Ti s.s) alloyed with Ni is formed at the Ti-Ni interface (see Fig. 4(a)). The joints bonded at 850 and 900°C, respectively, are composed of carbon steel/Ni/NiTi/remnant NiTi layers/Ti s.s/pure Ti, as can be seen in Figs. 4(b) and (c). We believe that this insight would be used as a valuable reference in expanding the use of Ti/Ni joints in construction or other fields.

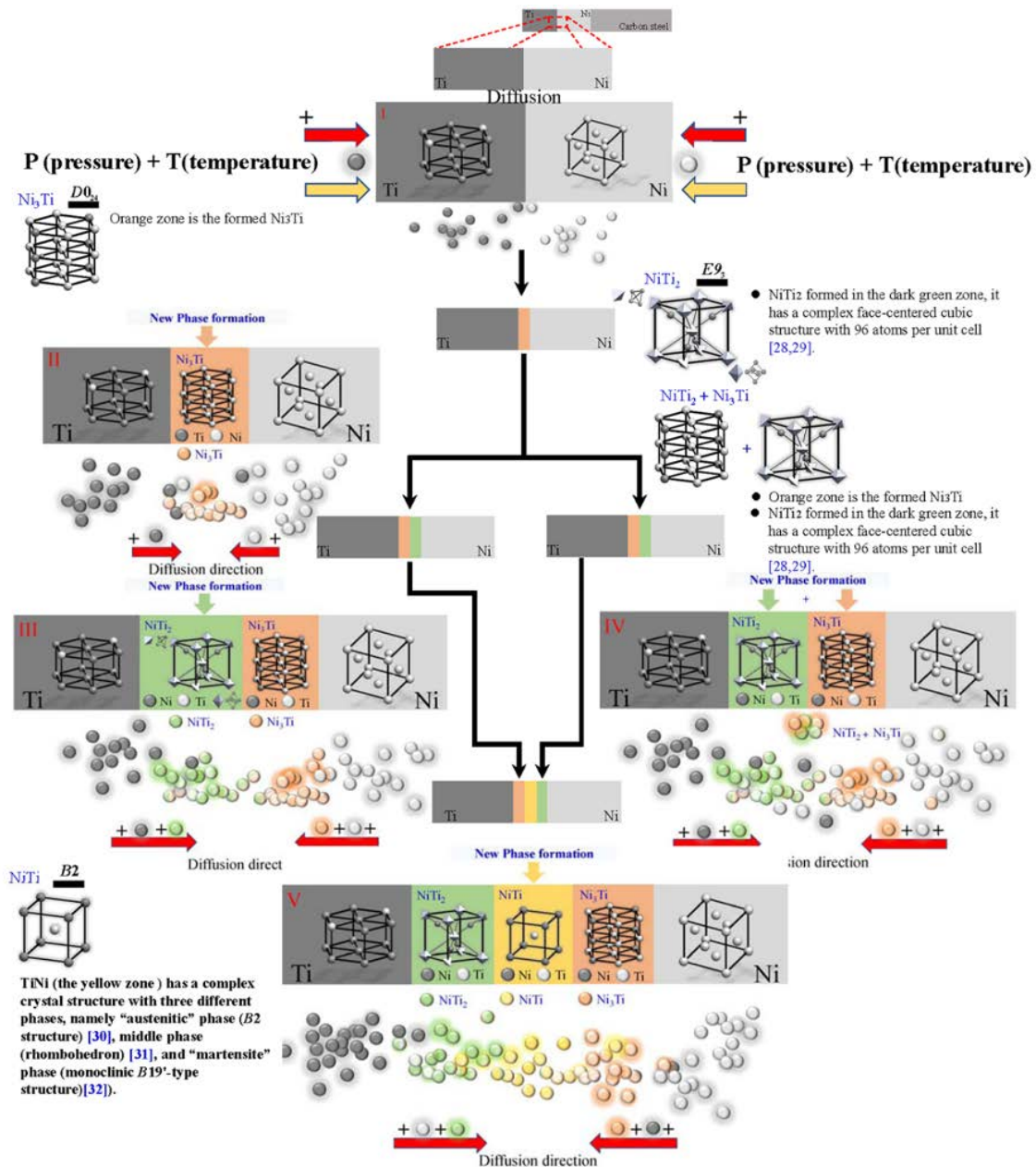


Fig. 3. Two possible compound formation sequences based on thermodynamic analysis results. (a) $Ni_3Ti \rightarrow NiTi_2 \rightarrow NiTi$ and (b) Ni_3Ti and $NiTi_2 \rightarrow NiTi$.

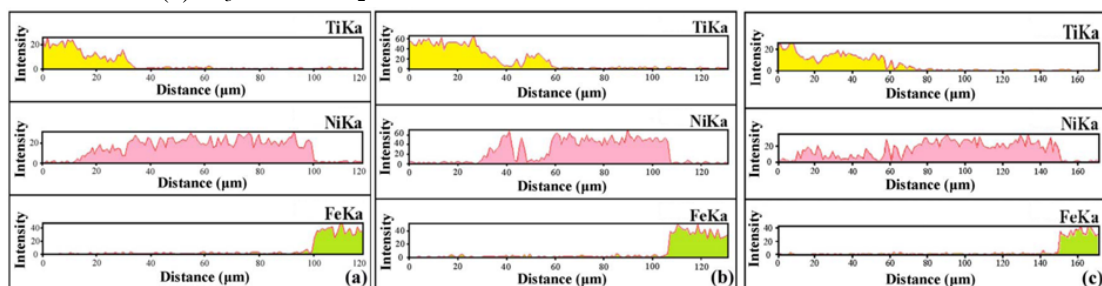


Fig. 4. Elemental concentration profiles of interfacial regions of pure Ti and carbon steel hot-roll diffusion bonded joints with Ni interlayer processed at temperatures of: (a) 800°C, (b) 850°C and (c) 900°C.

CONCLUSIONS

Commercially-pure Ti and carbon steel plates

have been bonded with a Ni interlayer at processing temperatures of 800, 850 and 900°C, respectively, using a hot-roll solid-state diffusion bonding technique. The compound joints were found to contain $NiTi_2$,

NiTi and Ni₃Ti compounds at the Ti-Ni diffusion interface. The two alternative possible formation sequences of the three compounds were investigated by thermodynamic analysis. The results showed the formation sequence to be Ni₃Ti → NiTi₂ → NiTi for the first possible phase formation. In other words, Ni₃Ti was formed at the beginning of the diffusion reaction process on the Ni side and was subsequently followed by the formation of NiTi₂ on the Ti side. Meanwhile, the second possible formation sequence is: Ni₃Ti → Ni₃Ti + NiTi₂ → NiTi. In particular, the second possible formation that the interface with Ni₃Ti and NiTi₂ forms almost simultaneously and is then followed by the formation of NiTi, can be attributed to the lower reaction Gibbs free energies and surface energy increments of Ni₃Ti and NiTi₂. However, the surface energy increments of Ni₃Ti and NiTi₂ are very similar. Consequently, it is also possible that Ni₃Ti and NiTi₂ nucleate first and NiTi then nucleates in the Ti-Ni diffusion int. Overall, both sets of results indicate an inter-diffusion of the two elements (Ti and Ni). The gradual increase in the Ti concentration from the Ti side to the Ni side of the Ti-Ni joint provides further evidence of diffusion in the bonding process. α + β Ti phases additionally exist as discrete needle-shaped particles in the matrix of the Ni₃Ti phase, while β-Ti phases exist as discrete islands in the matrix of the NiTi₂ phase. The atomic migration of chemical species across the bond line increases with an increasing bonding temperature. The presence of Ni in the interfacial zone adjacent to the Ti substrate stabilizes the β-Ti phase, leads to the formation of needle-shaped α + β-Ti phase, and acts as a diffusion barrier which prevents the migration of Ti atoms to the carbon steel substrate.

ACKNOWLEDGMENT

The authors would like to thank the Ministry of Science and Technology of Taiwan for the financial support of this study under Contract No. MOST 105-2218-E-027 -011-MY3.

REFERENCES

- Karolczuk, A., Kowalski, M., Bański, R., and Żok, F., "Fatigue phenomena in explosively welded steel-titanium clad components subjected to push-pull loading," *International Journal of Fatigue*, Vol. 48, pp.101-108 (2013).
- Weng, F., Chen, C., and Yu, H., "Research status of laser cladding on titanium and its alloys: A review," *Materials and Design*, Vol.58, pp.412-425 (2014).
- Lee, W. B., Lee, C. Y., Chang, W. S., Yeon, Y. M., and Jung, S. B., "Microstructural investigation of friction stir welded pure titanium," *Materials Letters*, Vol.59, No.26, pp.3315-3318 (2005).
- Sun, Z., Annergren, I., Pan, D., and Mai, T. A., "Effect of laser surface remelting on the corrosion behavior of commercially pure titanium sheet." *Materials Science and Engineering: A*, Vol.345 ,No.1-2, pp.293-300 (2003).
- Kahraman, N., Gulenc, B., and Findik, F., "Corrosion and mechanical-microstructural aspects of dissimilar joints of Ti-6Al-4V and Al plates," *International Journal of Impact Engineering*, Vol.34, No.8, pp.1423-1432 (2007).
- Zhao, D. S., Yan, J. C., Wang, Y., and Yang, S. Q., "Relative slipping of interface of titanium alloy to stainless steel during vacuum hot roll bonding," *Materials Science and Engineering: A*, Vol. 499, pp. 282-286 (2009).
- Borts, B. V., "Formation of the joint dissimilar metals in the solid phase by the method of vacuum hot rolling," *Materials Science*, Vol. 47, pp. 689-695 (2012).
- Zhao, D. S., Yan, J. C., and Liu, Y. J., "Effect of intermetallic compounds on heat resistance of hot roll bonded titanium alloy-stainless steel transition joint," *Transactions of Nonferrous Metals Society of China*, Vol. 23, pp. 1966-1970 (2013).
- Akramifard, H. R., Mirzadeh, H., and Parsa, M. H., "Cladding of aluminum on AISI 304L stainless steel by cold roll bonding: Mechanism, microstructure, and mechanical properties," *Materials Science and Engineering: A*, Vol. 613, pp. 232-239 (2014).
- Yang, D. H., Luo, Z. A., Xie, G. M., Wang, M. K., and Misra, R. D. K., "Effect of vacuum level on microstructure and mechanical properties of titanium-steel vacuum roll clad plates," *Journal of Iron and Steel Research International*, Vol. 25, pp. 72-80 (2018).
- Arik, H., Aydin, M., Kurt, A., and Turker, M., "Weldability of Al4C3-Al composites via diffusion welding technique," *Materials and design*, Vol. 26, pp. 555-560 (2005).
- Kundu, S., and Chatterjee, S., "Interfacial microstructure and mechanical properties of diffusion-bonded titanium-stainless steel joints using a nickel interlayer," *Materials Science and Engineering: A*, Vol. 425, pp. 107-113 (2006).
- Verdier, M., Groma, I., Flandin, L., Lendvai, J., Bréchet, Y., and Guyot, P., "Dislocation densities and stored energy after cold rolling of Al-Mg alloys: investigations by resistivity and differential scanning calorimetry," *Scripta Materialia*, Vol. 37, pp. 449-454 (1997)
- Shirzadi, A. A., & Wallach, E. R., "Analytical modelling of transient liquid phase (TLP) diffusion bonding when a temperature gradient is imposed," *Acta materialia*, Vol.47, No.13,

- pp.3551-3560 (1999).
- Oliveira, J. P., Cavaleiro, A. J., Schell, N., Stark, A., Miranda, R. M., Ocana, J. L., and Fernandes, F. B., "Effects of laser processing on the transformation characteristics of NiTi: A contribute to additive manufacturing," *Scripta materialia*, Vol. 152, pp. 122-126 (2018).
- Marattukalam, J. J., Balla, V. K., Das, M., Bontha, S., & Kalpathy, S. K., "Effect of heat treatment on microstructure, corrosion, and shape memory characteristics of laser deposited NiTi alloy," *Journal of Alloys and Compounds*, Vol. 744, pp. 337-346 (2018).
- Beres, J., Polar, A., and Indacochea, J. E., "Joining YSZ to 444 SS by in situ alloying in a Ni-Ti filler metal for SOFC applications," *In Proceeding of the 3rd international brazing and soldering conference. San Antonio: American Welding Society*, pp. 125-132 (2006).
- Okamoto, H., and Massalski, T. B., "Binary alloy phase diagrams," *ASM International, Materials Park* (1990).
- Hey, J. C., and Jardine, A. P., "Shape memory TiNi synthesis from elemental powders," *Materials Science and Engineering: A*, Vol. 188, pp. 291-300 (1994).
- Deng, Y., Sheng, G., and Xu, C., "Evaluation of the microstructure and mechanical properties of diffusion bonded joints of titanium to stainless steel with a pure silver interlayer," *Materials and Design*, Vol. 46, pp. 84-87 (2013).
- Orhan, N., Aksoy, M., and Eroglu, M., "A new model for diffusion bonding and its application to duplex alloys," *Materials Science and Engineering: A*, Vol. 271, pp. 458-468 (1999).
- Sam, S., Kundu, S., and Chatterjee, S., "Diffusion bonding of titanium alloy to micro-duplex stainless steel using a nickel alloy interlayer: Interface microstructure and strength properties," *Materials and Design*, Vol. 40, pp. 237-244 (2012).
- Kundu, S., Sam, S., and Chatterjee, S., "Interface microstructure and strength properties of Ti-6Al-4V and microduplex stainless steel diffusion bonded joints," *Materials and Design*, Vol. 32, pp. 2997-3003 (2011).
- Liu, J., Su, Y., Xu, Y., Luo, L., Guo, J., and Fu, H., "First phase selection in solid Ti/Al diffusion couple," *Rare metal materials and engineering*, Vol. 40, pp. 753 (2011).
- De Boer, F. R., Mattens, W., Boom, R., Miedema, A. R., and Niessen, A. K., "Cohesion in metals. Transition metal alloys," (1988).
- Kundu, S., Chatterjee, S., Olson, D., & Mishra, B., "Effects of intermetallic phases on the bond strength of diffusion-bonded joints between titanium and 304 stainless steel using nickel interlayer," *Metallurgical and materials transactions A*, Vol. 38, pp. 2053-2060 (2007).
- ASTM-D 1876-01 standards, *ASTM*, PA, (2015).
- Taylor, A., and Floyd, R. W., "Precision measurements of lattice parameters of non-cubic crystals," *Acta Crystallographica*, Vol. 3, pp. 285-289 (1950).
- Yurko, G. A., Barton, J. W., and Parr, J. G., "The crystal structure of Ti₂Ni," *Acta Crystallographica*, Vol. 12, pp. 909 (1959).
- Li, Y., Cui, L., Shi, P., and Yang, D., "Phase transformation behaviors of prestrained TiNi shape memory alloy fibers under the constraint of a hard substrate," *Materials Letters*, Vol. 49, pp. 224-227 (2001).
- Otsuka, K., & Ren, X., "Recent developments in the research of shape memory alloys," *Intermetallics*, Vol. 7, pp. 511-528 (1999).
- Fukuda, T., Kakeshita, T., Houjoh, H., Shiraiishi, S., and Saburi, T., "Electronic structure and stability of intermetallic compounds in the Ti-Ni system," *Materials Science and Engineering: A*, Vol. 273, pp.166-169 (1999).

熱軋擴散製程結合鈦-鎳-碳 鋼金屬複合 (Ti-Ni-steel) 薄 板探討擴散層形成及生成 順序

林俊銘

明新科技大學機械工程學系

摘要

本文旨在探討熱軋擴散製程對鈦-碳-鋼 (Ti-Ni-steel) 三金屬複合板的擴散層形成及生成順序。其結果，深入了解不同加工溫度對熱軋擴散結合的 Ti/Ni/steel 接合 Ti/Ni 界面演變的影響，以及對微觀結構觀察和熱力學計算揭示了一些有趣的結果。在擴散過程中，Ni₃Ti 和 NiTi₂ 幾乎同時開始形核；因此，兩層的厚度非常相似。最後，Ti 和 Ni 擴散到 NiTi₂ 和 Ni₃Ti 化合物層之間的界面，形成 NiTi。隨著 NiTi 層厚度的增加，部分 Ni₃Ti 被消耗掉；導致其厚度減小，這可歸因於較低的反應吉布斯自由能和 Ni₃Ti 和 NiTi₂ 的表面能增量。α + β Ti 相在 Ni₃Ti 相的基體中另外以離散的針狀顆粒形式存在，而 β-Ti 相在 NiTi₂ 相的基體中以離散的島狀存在。與 Ti 基體相鄰的界面區中 Ni 的存在穩定了 β-Ti 相，導致形成針狀 α + β-Ti 相。